communications biology

A Nature Portfolio journal

Article

https://doi.org/10.1038/s42003-025-07834-1

Melatonin affects trophoblast epithelial-to-mesenchymal transition and oxidative damage resistance by modulating GDF15 expression to promote embryo implantation

Guang Yang[1,2,3,5], Guidong Yao[1,2,3,4,5] ✉, Huihui Wang[1,2,3,5], Ran Jiang[1,2,3,5], Junnan Fang[1,2,3], Jingyi Hu[1,2,3], Yue Kong[1,2,3], Haixia Jin[1,2,3], Wenyan Song[1,2,3], Zhaoting Wu[1,2,3], Xianju Huang[1,2,3] & Yingpu Sun[1,2,3] ✉

Melatonin is widely observed in the female reproductive system and regulates trophoblast cell functions, but its effects on embryo implantation and underlying mechanisms are not well understood. By constructing an in vitro embryo culture model, we found that melatonin enhances migration and implantation in human and mouse trophoblast cells. It also significantly promoted HTR-8/SVneo cell proliferation, inhibited apoptosis, enhanced migration, and mitigated oxidative damage. Further investigation revealed that melatonin promoted trophoblast cell migration and increased the in vitro implantation rate of HTR-8/SVneo spheroids by promotes epithelial-mesenchymal transition (EMT) via the growth differentiation factor 15 (GDF15)–mothers against decapentaplegic homolog 2/3 (SMAD2/3) pathway. Additionally, melatonin increased the levels of glutathione peroxidase 4 (GPX4) and glutathione (GSH) in HTR-8/SVneo cells by upregulating the expression of GDF15, inhibiting reactive oxygen species (ROS) accumulation, and increasing mitochondrial membrane potential, thus suppressing apoptosis during oxidative stress. In conclusion, melatonin promotes EMT in trophoblast cells via GDF15-SMAD2/3 pathway and partially induces the expression of GPX4 through GDF15 to enhance oxidative damage resistance in trophoblast cells. These findings highlight melatonin's regulatory role in embryo implantation and suggest new avenues for exploring its biological effects in reproduction and clinical applications.

Embryo implantation is a critical step in ontogenesis, and good implantation marks the establishment of pregnancy and facilitates the provision of adequate nutritional support for fetal development. This process can be characterized as a molecular dialog jointly mediated by various cytokines, adhesion molecules, and matrix proteases[1]. Studies have shown that two-thirds of miscarriages are caused by implantation failure and that defective implantation can lead to the development of adverse pregnancy outcomes, such as infertility, intrauterine fetal growth restriction, and pre-eclampsia[2]. Therefore, in-depth investigations of the key molecules and signaling pathways involved in the implantation process are expected to improve the natural pregnancy rate and success rate of assisted reproductive technology, with broad translational potential and prospects for clinical applications.

The occurrence of epithelial-to-mesenchymal transition (EMT) in embryonic trophoblast cells is an important event for implantation. EMT is triggered when trophoblast cells come into contact with endometrial epithelial cells. At this point, the trophoblast cells lose polarity, exhibit enhanced migration and invasion, and acquire the strong ability to degrade

[1]Center for Reproductive Medicine, the First Affiliated Hospital of Zhengzhou University, Zhengzhou, China. [2]Henan Key Laboratory of Reproduction and Genetics, the First Affiliated Hospital of Zhengzhou University, Zhengzhou, China. [3]Henan Clinical Medical Research Center, Zhengzhou, China. [4]NHC Key Laboratory of Birth Defects Prevention, Zhengzhou, China. [5]These authors contributed equally: Guang Yang, Guidong Yao, Huihui Wang, Ran Jiang.
✉e-mail: ygdzzu@163.com; syp2008@vip.sina.com

the extracellular matrix[3], which helps the embryo implantation. More importantly, abnormal EMT of trophoblast is closely associated with miscarriage, pre-eclampsia, choriocarcinoma, and intrauterine growth restriction in pregnancy[4]. EMT is a complex, coordinated, and dynamic process that is influenced by many genetic and chemical factors.

Reactive oxygen species (ROS) are a class of highly reactive oxidizing molecules that include superoxide radicals and hydrogen peroxide, and they are widely observed in living organisms. ROS, in appropriate amounts, can participate in cell signaling, regulate cell physiological functions, and play a positive regulatory role in the processes of embryonic development and implantation. Excessive ROS, however, can penetrate the cell membrane and inhibit cell viability, causing cell cycle arrest at the S or G2/M phase, which damages embryo quality and endometrial receptivity[5,6] and alters the embryonic genome, thereby increasing the risk of diseases in adulthood and leading to transgenerational inheritance[7,8]. Currently, many factors exist that can expose embryos to high oxidative stress during development and implantation (e.g. in vitro culture systems, air pollution, or maternal obesity and aging). In addition to impairing the embryo's ability to attach to the endometrium, these factors can also result in further abnormalities in mitochondrial copy numbers within endometrial cells, which significantly contribute to the risk of miscarriages[9–11]. Hence, the proper function of the embryonic antioxidant system is crucial during implantation. Enhancing the ability of trophoblast cells to withstand oxidative damage and maintain optimal activity plays a key role in improving the success rate of embryo implantation.

Melatonin, a lipophilic hormone secreted primarily by the pineal gland, is released regularly over a 24-h period as a circadian rhythm regulator[12,13]. Studies have shown that expression of the melatonin synthase is gradually increased during early pregnancy in mice, and melatonin injection increases serum estradiol levels, the number of embryonic implantation sites, and the litter size[14–16]. Additional studies have shown that melatonin enhances the density of uterine glands[15], while embryo implantation sites are significantly diminished in aralkylamine *n*-acetyltransferase (AANAT) and melatonin receptor 2 (MT2) knockout mice, which exhibit abnormalities in uterine morphology and increased local inflammation[17]. Further, melatonin can reduce cell apoptosis[16], promote cell migration[18] and inhibit the oxidative stress-induced[19] in human trophoblast cells. However, current studies primarily focus on melatonin's role in improving endometrial receptivity, with few studies exploring the molecular mechanisms by which melatonin regulates trophoblast cell function during embryo implantation. This study aimed to investigate the role of melatonin during embryo implantation and the underlying molecular mechanisms, from the perspectives of both the melatonin-mediated regulation of trophoblast EMT and oxidative damage resistance.

Results

Melatonin enhances the embryo implantation rate by promoting trophoblast migration

To investigate the effect of melatonin on embryo implantation, we first used a human in vitro embryo implantation model. The results showed that the embryo implantation rate was significantly higher in the 10 μM melatonin treatment group than in the control group (70.00% vs. 47.50%, $p < 0.05$; Fig. 1A, B). To determine whether melatonin affects mouse embryo implantation, we obtained mouse E4.5 embryos co-cultured with the Ishikawa endometrial cell line for 48 h (Fig. 2A) and assessed the implantation of E5.5 embryos (Fig. 2B), trophoblast migration in E5.5 embryos (Fig. 2C), and the migration range of E6.5 trophoblast cells (Fig. 2D, E). The results showed that the implantation rate of E5.5 embryos was significantly higher in the 10 μM melatonin treatment group than in the control group (70.00% vs. 35.00%, $p < 0.05$; Fig. 2F), whereas the trophoblast migration rate did not differ significantly between the two groups (40.00% vs. 15.00%, $p > 0.05$; Fig. 2G); moreover, the migration range of E6.5 embryonic trophoblast cells in the 10 μM melatonin treatment group was significantly greater than that in the control group ($p < 0.05$; Fig. 2H).

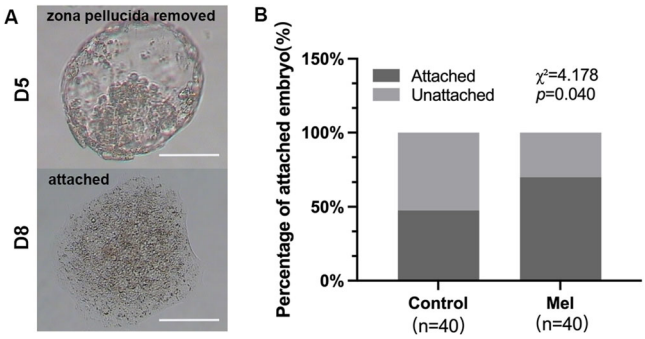

Fig. 1 | The in vitro implantation rate was promoted after melatonin treatment of human peri-implantation embryos. Human blastocysts were cultured in vitro and the morphology of the D5 blastocyst without zone pellucida and adherent D8 embryo were recorded (**A**). Statistical analysis of D8 embryo implantation rate was performed between melatonin (10 μM) treatment group ($n = 40$) and control group ($n = 40$) (**B**). Scale bar is 50 μm, $p < 0.05$ indicates significant difference.

Melatonin helps to promote the function of human trophoblast cells

To further investigate the mechanism underlying the effect of melatonin on embryo implantation, we used the human trophoblast cell line HTR-8/SVneo to examine how melatonin affects the function of trophoblast cells. Immunofluorescence staining showed that melatonin receptors MT1 and MT2 were both expressed in the HTR-8/SVneo cell line and were mainly observed in the cytoplasm, with a low level of expression in the nucleus (Supplementary Fig. 1). This suggests that melatonin can affect the functioning of trophoblast cells by binding to its receptors.

To clarify the effect of melatonin on the migration of HTR-8/SVneo cells, scratch assays were performed. The results showed that melatonin (10 μM) significantly increased the scratch healing rate ($p < 0.05$) compared to that in the control group (Fig. 3A, B). The results of transwell assays showed that melatonin (10 μM) treatment for both 6 and 12 h could significantly promote cell migration ($p < 0.0001$; Fig. 3C, D).

Cell proliferation assays revealed that treatment with 10 and 50 μM of melatonin significantly promoted the proliferation of HTR-8/SVneo cells ($p < 0.001$; Fig. 4A). Furthermore, staining with Ki-67, a marker of cell proliferation, showed an increased proportion of Ki-67-positive cells in the melatonin treatment group (Fig. 4B). Cell cycle phase distribution was further examined using flow cytometry, and the results showed that melatonin significantly affected changes in the HTR-8/SVneo cell cycle (Fig. 4C, D). This was mainly reflected by the significantly higher proportion of S-phase cells for all concentrations of melatonin treatments ($p < 0.05$; Fig. 4E). Moreover, the results of the apoptosis assay showed that the proportions of early and intermediate apoptotic cells were reduced (Fig. 4F), whereas the apoptotic index decreased as the melatonin concentration was increased, with 50 μM melatonin treatment resulting in significant reductions ($p < 0.01$; Fig. 4G).

To determine whether melatonin could improve the oxidative stress resistance of HTR-8/SVneo cells, we first examined the effects of different concentrations of melatonin treatment on the cellular ROS levels. The results showed that 10 μM melatonin significantly downregulated cellular ROS levels ($p < 0.05$; Fig. 5A). In the H_2O_2-induced cellular oxidative stress model, treatment with 800 μM of H_2O_2 for 2 h significantly upregulated ROS levels and inhibited cell viability in HTR-8/SVneo cells ($p < 0.0001$; Fig. 5B, C), while melatonin pretreatment for 24 h significantly reduced the ROS level induced by H_2O_2, and this effect was dose-dependent ($p < 0.001$; Fig. 5D). Flow cytometry was further used to clarify the melatonin (10 μM) could alleviate the increase in ROS induced by H_2O_2 (800 μM; Fig. 5E–I).

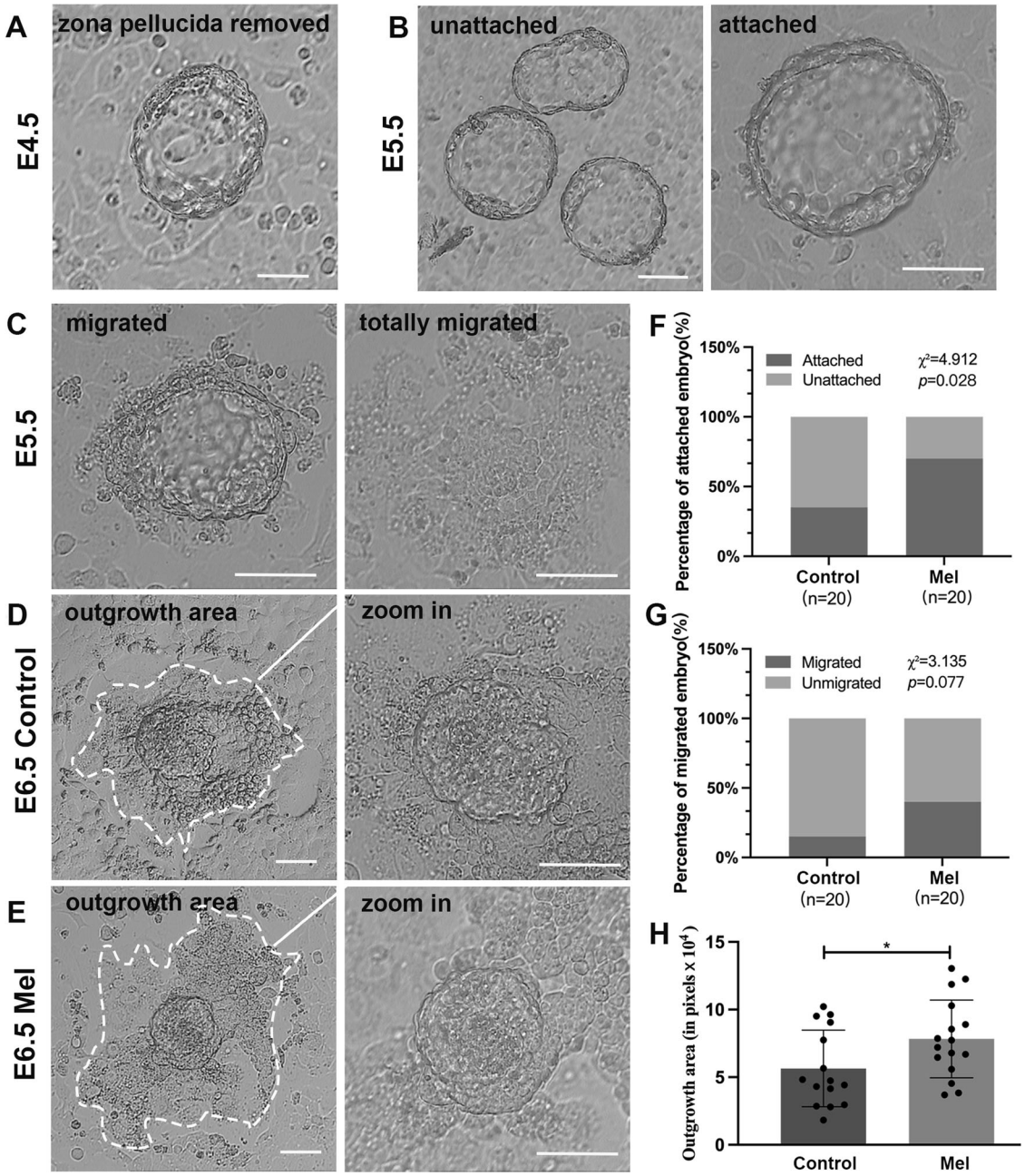

Fig. 2 | Mouse embryo implantation and trophoblast cell migration were promoted after melatonin treatment in vitro. Mouse E4.5 embryos were randomly assigned to the melatonin group (10 μM, $n = 20$) and the control group ($n = 20$) and co-cultured with the Ishikawa cells (**A**). Embryonic attachment (**B**) and trophoblast cell migration (**C**) were assessed at E5.5. The migration range of embryonic trophoblast cells in the control group (**D**) and the melatonin treated group (**E**) were evaluated at E6.5. The white dotted line is the independent boundary. Statistical analysis of E5.5 embryo implantation rate (**F**), E5.5 embryo migration rate (**G**), and E6.5 trophoblast cell migration range (**H**). Error bars indicate standard deviation (SD). Scale bar is 50 μm, * indicates $p < 0.05$.

Probing the molecular mechanisms by which melatonin affects HTR-8/SVneo cell functions using transcriptome sequencing

To investigate the molecular mechanisms by which melatonin affects the functioning of HTR-8/SVneo cells, we performed transcriptome sequencing on melatonin-treated HTR-8/SVneo cells. The results revealed a total of 864 differentially expressed genes (DEGs) in melatonin-treated HTR-8/SVneo cells compared to levels in the control group, of which, 387 genes were upregulated and 477 genes were downregulated. The heatmap showed several DEGs between the groups. Among these, the significantly elevated expression of *GDF15*, *HLA-C*, and *IGFBP2* was closely related to cellular functions and embryonic development; *SOD1*, *GPX1*, and *GPX4* were closely related to oxygen radical scavenging; and *NDUFB3*, *SIRT3*, and *MT-TH*, among others, were closely related to mitochondrial function (Fig. 6A). A volcano plot was used to visualize the overall distribution of DEGs between the two groups (Fig. 6B), and principal component analysis was further performed. Although there were differences between samples within the same group, the results of dimensionality reduction indicate that the melatonin group tended to be separated from the control group (Fig. 6C).

The functions of the DEGs were further analyzed via GO and KEGG pathway enrichment analysis. The results of GO analysis showed that DEGs were mainly enriched in cellular oxidative phosphorylation and mitochondrial functions, such as antioxidant enzyme activity, mitochondrial respiratory chain assembly, mitochondrial gene expression, ROS scavenging, and ATP generation, among others. Changes in cell adhesion

functions, such as cadherin binding, cellular tight junctions, and cell adhesion, and changes in cell polarity were enriched based on the DEGs. In addition, the functions of a few DEGs were directly related to embryo development and embryo implantation (Fig. 6D). KEGG analysis of the DEGs revealed that the functions were mainly focused on cellular metabolic pathways, such as cellular oxidative phosphorylation, cellular tight junctions, the cell cycle, the tricarboxylic acid cycle, and nucleic acid metabolism (Fig. 6E). Similarly, results from the gene set enrichment analysis of RNA expression profiles suggested that gene sets related to oxidative phosphorylation, mitochondrial protein translation, and ROS scavenging were more highly expressed in melatonin-treated HTR-8/SVneo cells. This implies that melatonin might reduce the cytotoxic effects of ROS by affecting mitochondrial functions and antioxidant enzyme activities (Fig. 6F).

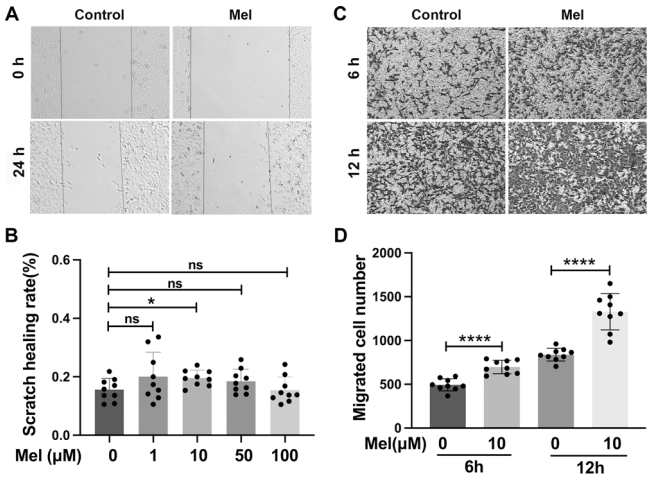

Fig. 3 | HTR-8/SVneo cell migration was promoted after melatonin treatment. Cell scratch experiments were used to stain the cell migration ability of the HTR-8/SVneo cell line after treatment with melatonin (10 μM) for 24 h (**A**). The scratch treatment rates of each group were statistically analyzed and compared (**B**). The Transwell chamber was used to detect the cell ability of migration in the HTR-8/SVneo cell line after treatment with melatonin for 6 h and 12 h (**C**), and statistically analyzed was performed (**D**). Ns indicates no significant difference, * indicates $p < 0.05$, **** indicates $p < 0.0001$.

Melatonin regulates EMT in HTR-8/SVneo cells through the GDF15–SMAD3 pathway

To investigate the pathway by which melatonin affects trophoblast migration, we incorporated the sequencing results to examine the mechanism underlying the regulatory effect of melatonin on EMT. The sequencing results suggested that melatonin can significantly increase the expression of GDF15. Previous studies have shown that GDF15 exerts its biological effect by activating the SMAD pathway, which in turn is closely related to EMT[20]. Therefore, we first examined the protein expression levels of GDF15, SMAD pathway-related proteins, and the key EMT molecules E-CAD and N-CAD (Fig. 7A). The results showed that melatonin (10 μM) significantly promoted the protein expression of GDF15, SMAD2/3, p-SMAD3, and N-CAD in HTR-8/SVneo cells ($p < 0.05$; Fig. 7A and Supplementary Fig. 2A–D), had a significant inhibitory effect on the expression of E-CAD ($p < 0.05$; Fig. 7A and Supplementary Fig. 2E), and had no significant effect on the protein expression of SMAD1/5 and p-SMAD1/5 ($p > 0.05$; Fig. 7A and Supplementary Fig. 2F). These results suggest that melatonin can promote GDF15 protein expression in trophoblast cells, activate the SMAD2/3 pathway, and alter the expression of cellular EMT-related molecules.

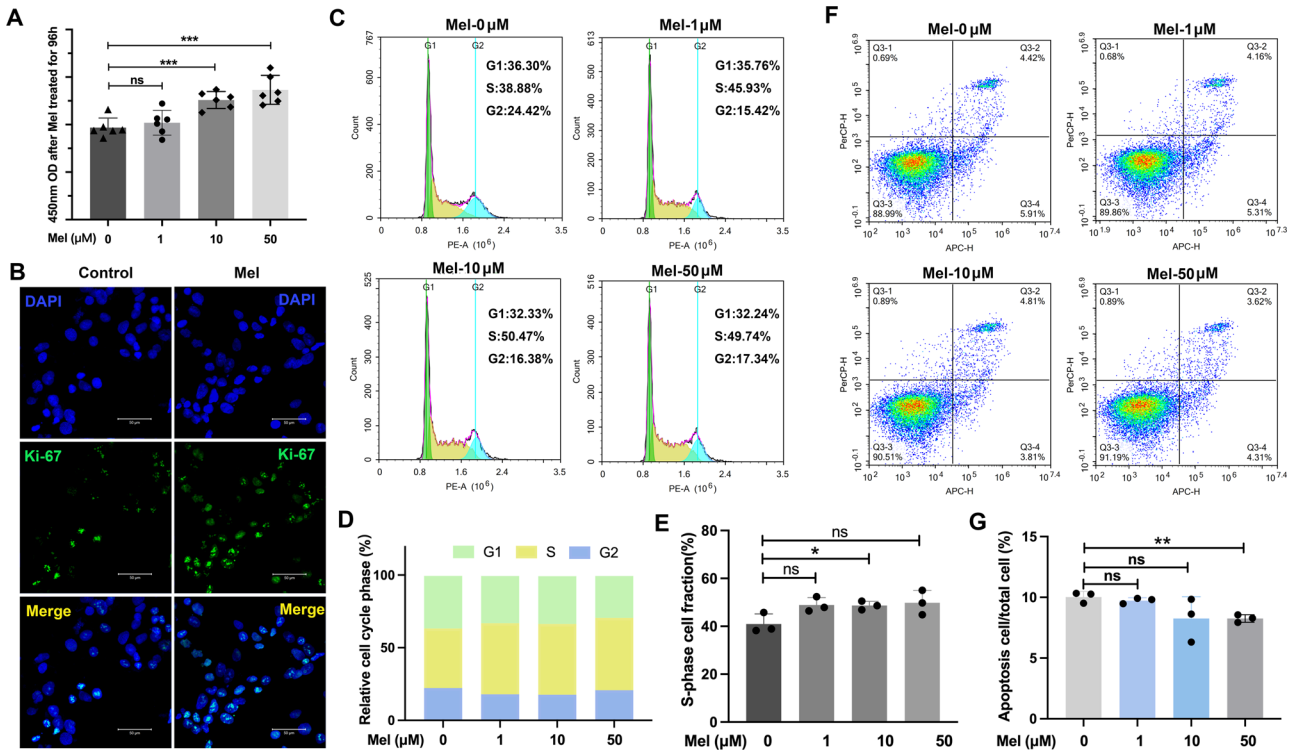

Fig. 4 | Melatonin promotes cell proliferation and inhibits apoptosis by affecting the cell cycle. CCK8 was used to determine the proliferation of HTR-8/SVneo cells after treatment with different concentrations of melatonin for 96 h (**A**). Ki-67 expression was detected by immunofluorescence after treatment with melatonin (10 μM) (**B**). Blue fluorescence represents nuclear localization, and green fluorescence is the expression signal of Ki-67. Flow cytometry was used to detect the effect of melatonin treatment for 24 h on the cell cycle of HTR-8/SVneo (**C**). The effects of different concentrations of melatonin on the cell cycle was compared (**D**), and statistically analyze the proportion of S-phase cells in each group was performed (**E**). Flow cytometry was used to detect the cell apoptosis of HTR-8/SVneo cells after treated with melatonin at different concentrations for 24 h (**F**), and the cell apoptosis index of each treatment group was statistically analyzed (**G**). Among them, Apoptosis index = (number of early apoptotic cells+ number of mid-stage apoptotic cells)/total number of cells. Ns indicates no significant difference, * indicates $p < 0.05$, ** indicates $p < 0.01$, *** indicates $p < 0.001$.

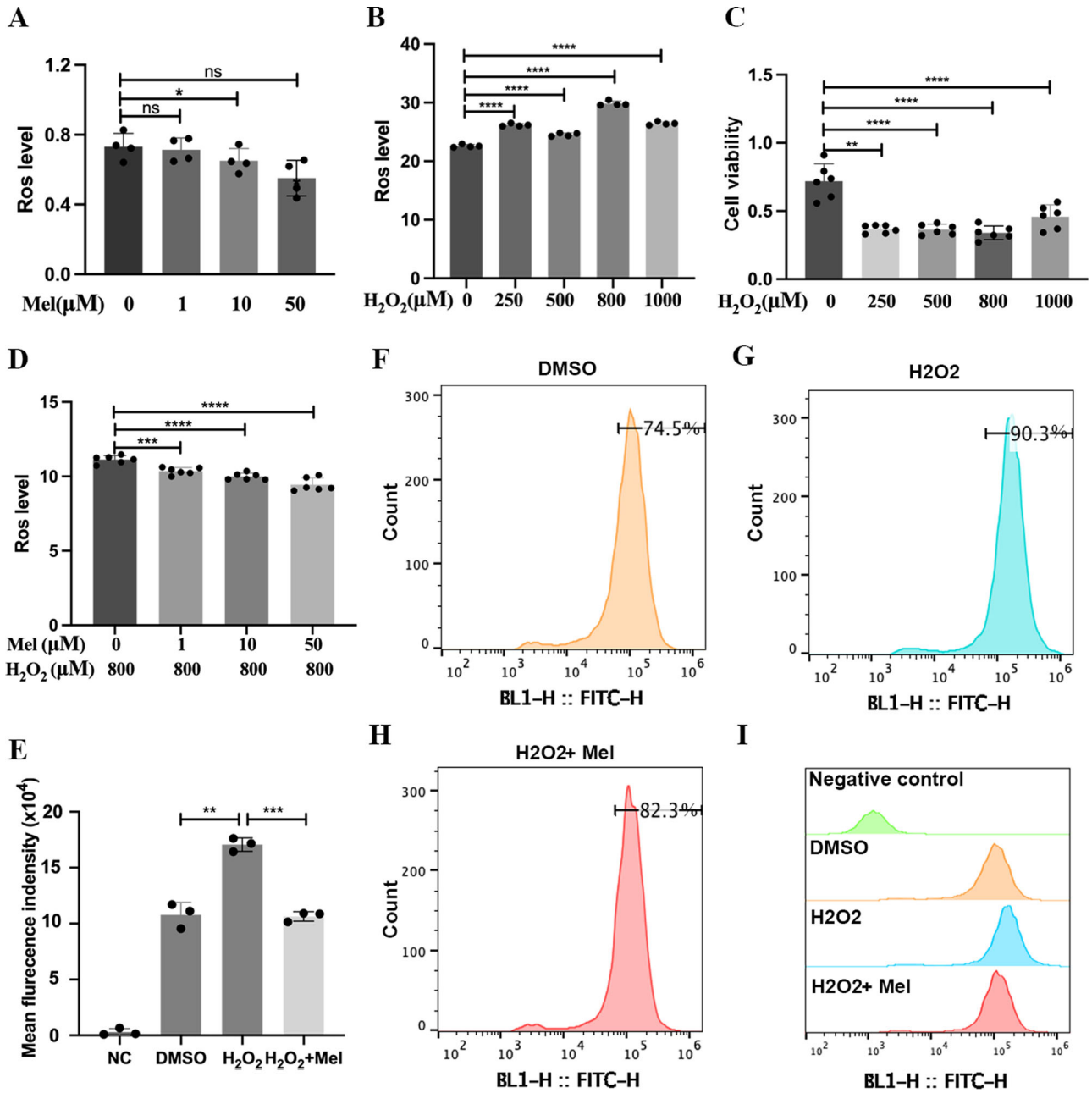

Fig. 5 | Melatonin can attenuate H_2O_2-induced oxidative stress damage in HTR-8/SVneo cells. A microplate reader was used to detect ROS levels in HTR-8/SVneo cells after treatment with different concentrations of melatonin for 24 h (**A**) or H_2O_2 for 2 h (**B**). Cell viability was detected after treatment with each concentration of H_2O_2 for 2 h (**C**). The cellular ROS levels was detected in cells after the treatment of different concentrations of melatonin for 24 h and 800 μM H_2O_2 for another 2 h (**D**). Flow cytometry was used to detect the ROS levels of cells in each treatment group, and the ROS fluorescence intensity was statistically analyzed (**E**–**I**). Ns indicates no statistical difference, * indicates $p < 0.05$, ** indicates $p < 0.01$, *** indicates $p < 0.001$, **** indicates $p < 0.0001$.

To further clarify the regulatory role of GDF15 in EMT in HTR-8/SVneo cells, we used three siRNAs targeting different regions of *GDF15* and assessed their knockdown efficiency at both the RNA and protein level (Fig. 7B and Supplementary Fig. 2G, H). The results showed that all three siRNAs had good knockdown effects ($p < 0.01$), and since si-GDF15-2 had the best knockdown effect, this siRNA was used in all subsequent experiments. After GDF15 knockdown, the expression levels of SMAD2/3, p-SMAD3, and N-CAD were significantly inhibited ($p < 0.05$), but there was no significant change in E-CAD ($p > 0.05$; Fig. 7B and Supplementary Fig. 2I–L). After GDF15 knockdown, the addition of melatonin did not significantly upregulate the expression levels of GDF15, SMAD2/3, p-SMAD3, and N-CAD ($p > 0.05$; Fig. 7C and Supplementary Fig. 2M–P), and the inhibitory effect of melatonin on the expression of E-CAD was suppressed ($p < 0.05$; Fig. 7C and Supplementary Fig. 2Q). These results suggest that the effect of melatonin on the expression of EMT-related proteins in HTR-8/SVneo cells might be GDF15-dependent.

To clarify whether SMAD3 is involved in the regulatory effect of melatonin on EMT, SIS3 (5 μM) was used to inhibit SMAD3 protein phosphorylation in HTR-8/SVneo cells. The results showed that following the significant inhibition of SMAD3 phosphorylation ($p < 0.05$), the expression of SMAD2/3 in HTR-8/SVneo cells was not significantly affected ($p > 0.05$), but N-CAD expression was significantly reduced ($p < 0.01$), whereas E-CAD expression was significantly elevated ($p < 0.01$). In addition, the expression levels of SMAD2/3, p-SMAD3, N-CAD, and E-CAD in the melatonin +SIS3 group did not differ significantly compared to those in the SIS3 group ($p > 0.05$; Fig. 7D and

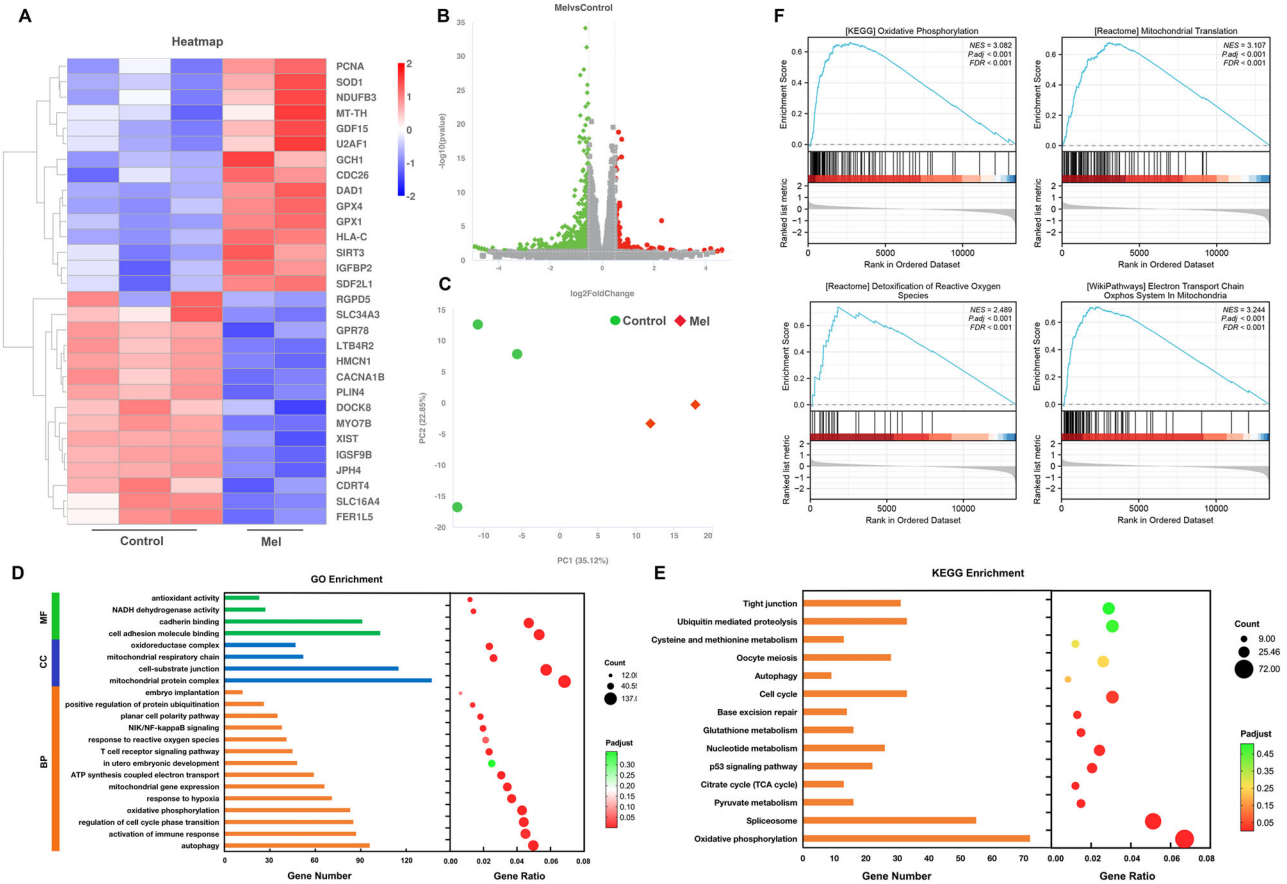

Fig. 6 | Analysis of DEG after melatonin treatment of HTR-8/SVneo cells. HTR-8/SVneo cells were treated with melatonin (10 μM) for 6 h and then subjected to transcriptome sequencing. The heat map shows significantly differentially expressed mRNA between groups (**A**). Each column represents a sample and each row represents a gene. The left side is a dendrogram of gene clustering and the module diagram of the subclusters. The right is the name of the gene. The volcano plot shows the initial differential expression of genes (**B**). The abscissa is the differential expression fold $\log_2$FC of the gene between the two samples. The ordinate is the statistical test value of the change in gene expression −log10 (*p*-value). Red dots represent significantly up-regulated genes, green dots represent significantly down-regulated genes, and gray dots represent non-significantly different genes. PCA was used to perform cluster analysis on samples (**C**). The horizontal axis represents the contribution of PC1 in the two-dimensional map to distinguishing samples, and the vertical axis represents the contribution of PC2 in the two-dimensional map to distinguishing samples. The red dots represent the melatonin group samples, and the green dots represent the control group samples. GO analysis was performed to enrich the function of differentially expressed mRNA (**D**). The vertical axis represents the GO term, the horizontal axis represents the number of genes or gene proportions, the size of the point represents the number of genes in the GO term, the color of the point represents *p* values, and the redder the color, the more significant the difference. BP, biological process; CC, cellular component; MF, molecular function. KEGG was used to analyze the signaling pathways involved in differentially expressed mRNAs (**E**). The vertical axis represents the sample name, the horizontal axis represents the number of genes or gene proportions, the size of the dots represents the number of genes enriched in this pathway, and the color of the dots corresponds to different *p* values. Gene set enrichment analysis of RNA expression profiles was performed after melatonin treatment of HTR-8/SVneo cells (**F**). NES, normalized enrichment score, NES positive and negative indicate higher and lower expression, respectively. $p < 0.05$ indicates significant difference.

Supplementary Fig. 2R-U). Thus, the promoting effect of melatonin on EMT in trophoblast cells is dependent on the phosphorylation of the SMAD3 protein.

To verify the regulatory role of the melatonin–GDF15–SMAD3 pathway in the adhesion function of trophoblast cells, HTR-8/SVneo cells were cultured in low-attachment 96-well plates until spheroids were formed. Then, the spheroids were co-cultured with the Ishikawa cell line (Fig. 7E), and the spheroid implantation rates were measured at 0.5 and 2 h. The results showed that melatonin had no significant effect on the implantation rate of trophoblast spheroids when co-cultured for 0.5 h ($p > 0.05$). However, when co-cultured for 2 h, melatonin significantly promoted the implantation of trophoblast spheroids ($p < 0.01$), but this promotive effect was significantly suppressed ($p < 0.05$) after GDF15 knockdown (Fig. 7F). Similarly, when co-cultured for 2 h, the promoting effect of melatonin on trophoblast cell implantation was significantly inhibited by SIS3 ($p < 0.001$; Fig. 7G). Furthermore, the marked increase in HTR-8/SVneo cell migration induced by melatonin ($p < 0.0001$) was significantly reversed after the knockdown of GDF15 expression or inhibition of SMAD3 protein phosphorylation ($p < 0.001$; Fig. 7H–J).

Melatonin participates in mouse embryo implantation in vivo via the GDF15 pathway

To further validate the aforementioned results, plug-positive mice were injected with melatonin and its receptor inhibitors for seven consecutive days. Embryo implantation was observed, and the number of implantation sites was determined at E7.5. Compared to that in the control group, significantly less implantation sites were observed in the Luzindole-injected (melatonin receptor inhibitor) group ($p < 0.05$; Fig. 8A, B). The localization of GDF15, E-CAD, and N-CAD expression was analyzed via the immunohistochemical staining of E7.5 decidua and embryonic tissues. The results showed that GDF15 was expressed in the decidua and all embryonic germ layers, whereas E-CAD and N-CAD were mainly expressed in embryonic trophoblast cells (Fig. 8C). In addition, the expression levels of GPX4, N-CAD, GDF15, p-SMAD3, and SMAD2/3 proteins were elevated in embryos

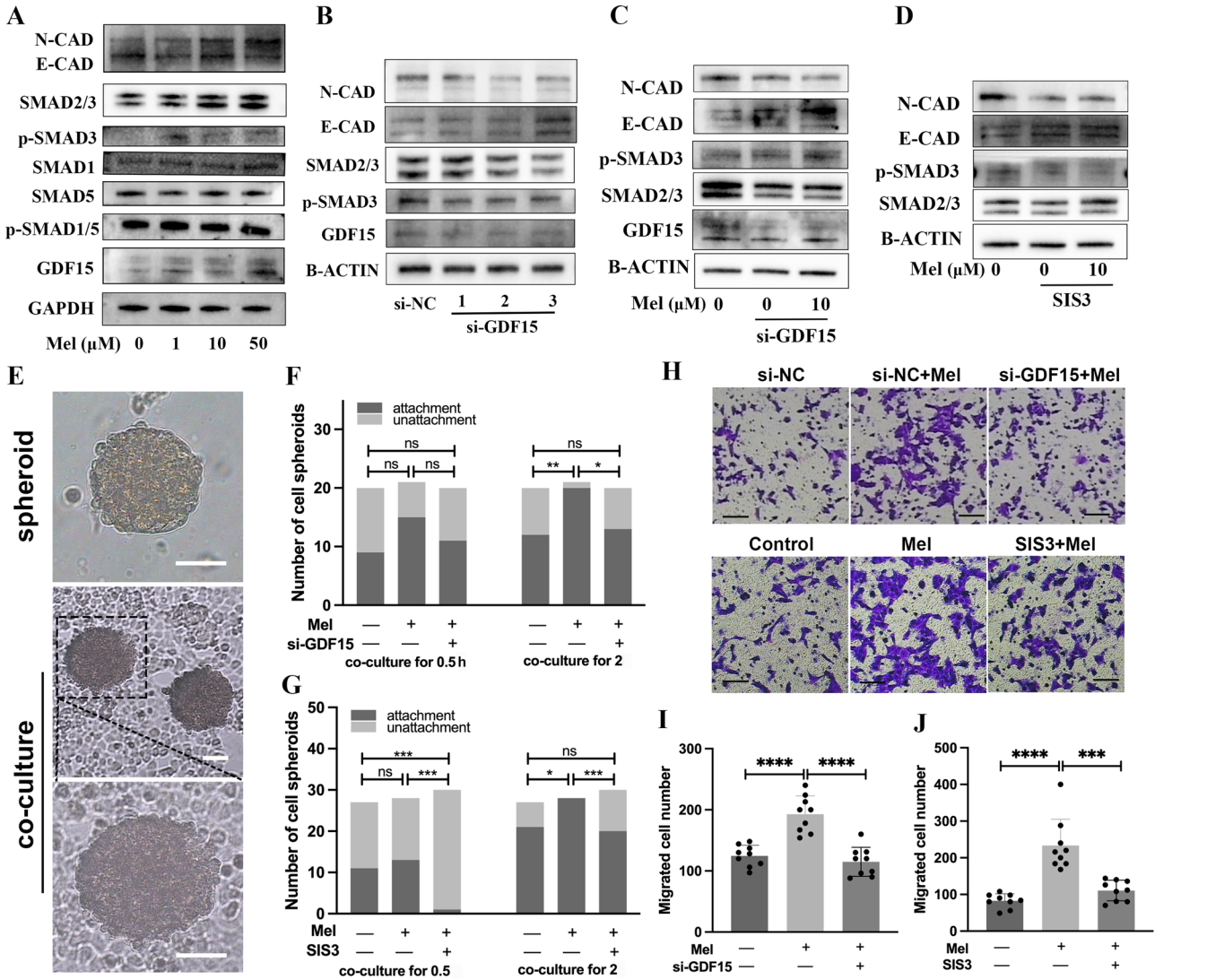

Fig. 7 | Melatonin regulates EMT through the GDF15-SMAD3 pathway to promote trophoblast cell transplantation and migration. After HTR-8/SVneo cells treated with different concentrations of melatonin for 24 h, the protein expression of GDF15, SMAD1, SMAD5, SMAD2/3, p-SMAD3, p-SMAD1/5, E-CAD, and N-CAD was detected (**A**). The protein expression of GDF15, SMAD2/3, p-SMAD3, E-CAD and N-CAD was detected after GDF15 knockdown treatment (**B**). After knocking down the expression of GDF15, melatonin (10 μM) was added again for 24 h to detect the protein expression of GDF15, SMAD2/3, p-SMAD3, E-CAD, and N-CAD (**C**). SIS3 (5 μM) was used for 6 h to inhibit SMAD3 protein phosphorylation and then add melatonin (10 μM) again for another 24 h to detect the protein expression of SMAD2/3, p-smad3, E-CAD and N-CAD (**D**). B-ACTIN/GAPDH is the internal reference protein. HTR-8/SVneo was cultured in a low-attachment 96-well plate for 24 h to form cell spheroids and co-cultured with ishikawa (**E**), and analyze the number of trophoblast cell spheres planted in each group at 0.5 h and 2 h (**F**, **G**). Transwell migration assay was used to detect the migration ability of cells in each group (**H**), and statistically analyzed the number of migrating cells in each group (**I**, **J**). Scale bar is 50 μm. Ns indicates no statistical significance, * indicates $p < 0.05$, ** indicates $p < 0.01$, *** indicates $p < 0.001$, **** indicates $p < 0.0001$.

of the melatonin group and reduced in those of the melatonin receptor inhibitor group, whereas the expression of E-CAD was reduced in the melatonin group and elevated in the inhibitor group (Fig. 8D).

Melatonin attenuates oxidative damage and inhibits apoptosis via the GDF15–GPX4 pathway

Melatonin has potent antioxidant effects, and our sequencing results suggested that it modulates mitochondrial functions and enhances antioxidant enzyme activity in HTR-8/SVneo cells. Therefore, we further explored whether GDF15 is involved in the antioxidant regulatory effects of melatonin on HTR-8/SVneo cells. Our findings demonstrated that expression levels of the antioxidant proteins GPX4 were altered to varying degrees after treatment with different concentrations of melatonin (Fig. 9A), and significant increases were observed in the 10 μM melatonin gourp ($p < 0.01$; Supplementary Fig. 3A), which was consistent with the sequencing results described previously herein. The expression level of GPX4 was significantly downregulated after GDF15 knockdown ($p < 0.05$; Fig. 9B and Supplementary Fig. 3B), and the upregulation of GPX4 expression induced by melatonin could be significantly attenuated by GDF15 knockdown (Fig. 9C and Supplementary Fig. 3C), suggesting that melatonin upregulated the expression of GPX4 via the GDF15 pathway. Since GSH was observed to be an important molecule affecting GPX4 activity, we examined its levels in HTR-8/SVneo cells. The results showed that melatonin significantly increased intracellular GSH levels ($p < 0.01$) and significantly reversed the H_2O_2-induced decrease in GSH levels ($p < 0.0001$; Fig. 9D). Moreover, the melatonin-induced increase in GSH levels could be partially attenuated by GDF15 knockdown ($p < 0.0001$; Fig. 9E).

We further employed a cellular oxidative stress model to explore the effects of the melatonin–GDF15 pathway on oxidative damage resistance. Melatonin attenuated the H_2O_2-induced increase in ROS in HTR-8/SVneo cells ($p < 0.05$), and this effect could be partially attenuated by GDF15 knockdown (Fig. 9F, G). In addition, melatonin mitigated the decrease in

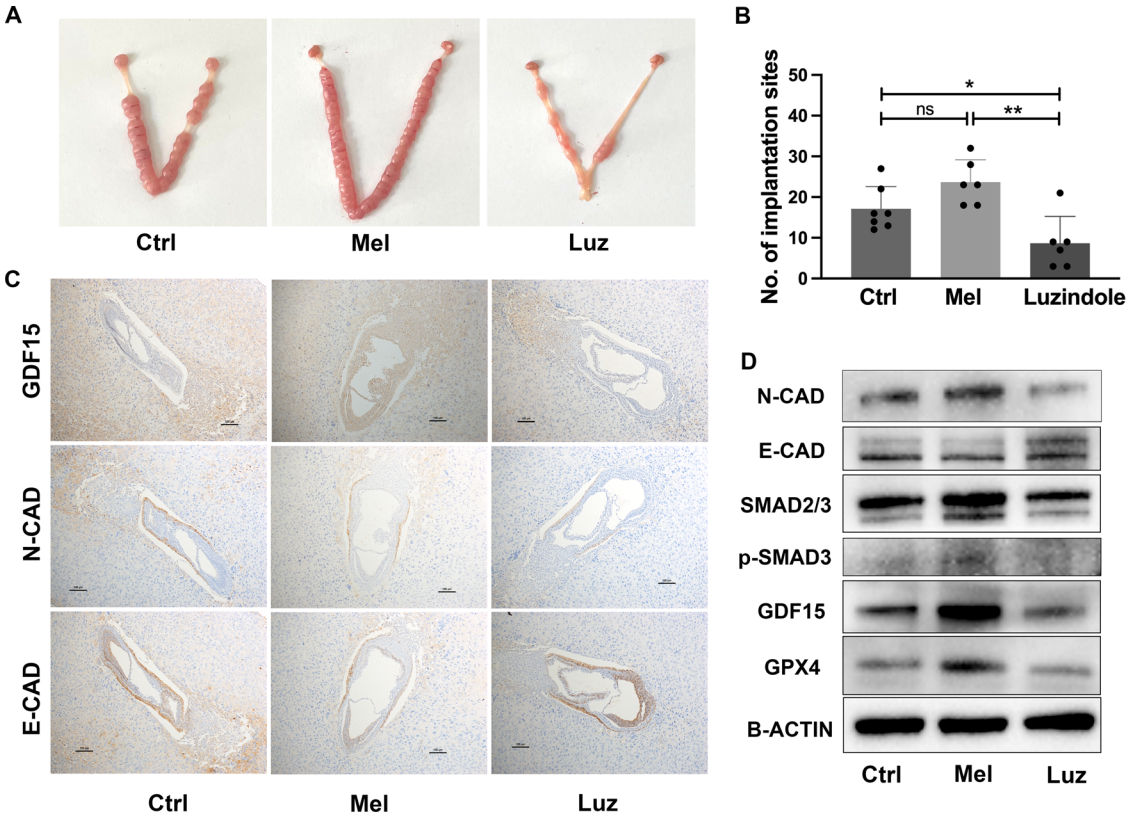

Fig. 8 | The mouse in vivo embryo implantation model was used to explore the involvement of GDF15 pathway in the regulation of embryo implantation by melatonin. Melatonin (10 mg/kg) and luzindole (1 mg/kg) were injected intraperitoneally into the mice on the day the plug was seen for 7 days. The uterus was harvested at E7.5 and the embryos were collected. Observe the embryo implantation sites of mice in each group (**A**), and perform statistical analysis on the number of uterine implantation sites (**B**). Immunohistochemical stain was used to analyze the localization and expression of GDF15, N-CAD and E-CAD in E7.5 embryonic and decidual tissues of mice in each group (**C**). E7.5 mouse embryos from each group were obtained and the protein expression levels of GPX4, GDF15, p-SMAD3, SMAD2/3, N-CAD and E-CAD were detected (**D**) B-ACTIN was the internal reference protein. Ns indicates no statistical significance, * indicates $p < 0.05$, ** indicates $p < 0.01$.

mitochondrial membrane potential caused by H_2O_2 ($p < 0.05$), and the protective effect of melatonin on mitochondrial membrane potential was reduced following the downregulation of GDF15 expression (Fig. 9H–K). Similarly, electron microscopy results showed that the protective effects of melatonin on mitochondrial morphology ($p < 0.05$) (e.g., melatonin-mediated mitigation of H_2O_2-induced mitochondrial swelling, cristae disappearance, membrane rupture, etc.) were reduced following the downregulation of GDF15 expression (Fig. 9L, M). Finally, apoptosis assays showed that melatonin significantly alleviated H_2O_2-induced apoptosis ($p < 0.001$), and this effect was significantly decreased by the downregulation of GDF15 expression (Fig. 9N, O). These results suggest that the GDF15–GPX4 axis is a key pathway for the melatonin-mediated regulation of oxidative damage resistance in trophoblast cells.

Discussion

Trophoblast cells differentiate from the embryo at the blastocyst stage and interact with maternal endometrial cells on days 6–8 after fertilization to promote embryo implantation. The process of embryo implantation involves the regulation of trophoblast cell functions, mediated by different cell growth factors and hormones, but many questions remain unanswered regarding this process.

Melatonin influences the hypothalamic–pituitary–gonadal axis to regulate gonadotropin secretion and exhibits various biological functions through both receptor-dependent and independent mechanisms[21–23], thereby playing a crucial role in processes such as gamete protection, embryo development, and maternal–fetal interactions[24]. Under physiological conditions, melatonin maintains high concentrations in the female reproductive system, with a concentration of 300 pg/mL in follicular fluid[25] and 30–40 pg/mL in fallopian tube fluid[26], and the melatonin levels in serum further increase during pregnancy[15]. Additionally, melatonin receptors (MT1 and MT2) and synthesizing enzymes, including AANAT and hydroxyindole O-methyltransferase (HIOMT), are widely expressed in the placenta and the trophoblast layer of chorionic villi, facilitating the effective synthesis of melatonin within the uterus[27,28]. These strongly indicates its paracrine or autocrine roles in placental function and embryo development[29,30].

In in vitro experiments, treatment with melatonin at concentrations of 10–100 μM can effectively reduce oxidative stress and promote the developmental potential of oocytes and embryos[31–34]. For trophoblast cells, 10 pM to 1 mM melatonin enhances the formation of syncytiotrophoblasts and increases the secretion of β-hCG[35], and 1 mM melatonin also protects human primary villous trophoblasts from autophagy, inflammation, and apoptosis[36]. In our study, we found that the exogenous addition of melatonin at concentrations ranging from 1 to 50 μM can exert biological effects without accompanying toxic reactions, with 10 μM significantly promoting embryo adhesion and trophoblast cell migration, while inhibiting cell apoptosis. The concentration of melatonin exerting effects in vitro is higher than physiological levels, which may be due to the following reasons: (1) cells exchange with blood to maintain melatonin levels in vivo, but this does not occur in cultured cells, so higher concentrations are needed to stabilize the drug's effects; (2) higher concentrations in cell studies enhance biological effects, making results more measurable; (3) in vitro experiments are typically of short duration and cannot simulate the long-term metabolism and distribution of drugs in vivo. Therefore, higher concentrations help to exert the drug's effects within a shorter time.

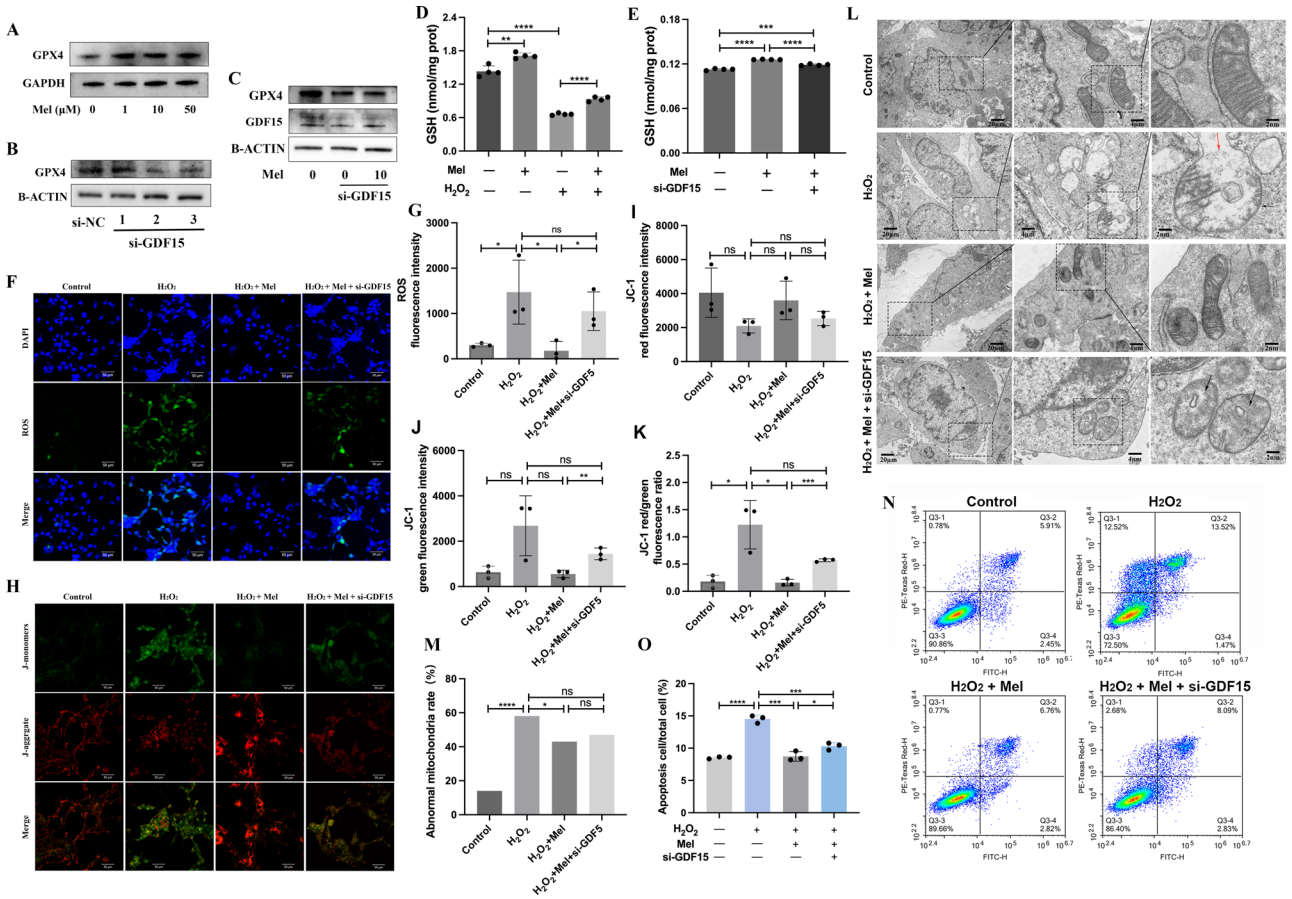

Fig. 9 | The GDF15-GPX4 pathway is involved in the regulation of the antioxidant effects of melatonin on HTR-8/SVneo cells. The protein expression levels of GPX4 was detected after HTR-8/SVneo cells were treated with melatonin (10 μM) for 24 h (**A**). The protein expression of GPX4 was detected after the treatment of si-GDF15 (**B**) and the co-treatment of melatonin and si-GDF5 (**C**). B-ACTIN/GAPDH was an internal protein. H_2O_2 (800 μM, 2 h) was used to induce oxidative stress in HTR-8/SVneo cells, and the intracellular GSH level after melatonin treatment was detected (**D**). After knocking down GDF15, GSH levels in HTR-8/SVneo cells were detected after melatonin treatment for 24 h (**E**). Fluorescent stain was used to detect the effects of melatonin and GDF15 on ROS levels in HTR-8/SVneo cells (**F**, **G**). Blue fluorescence represents the nuclear signal, and green represents the ROS signal. Fluorescent stain was used to detect the effects of melatonin and GDF15 on mitochondrial membrane potential in HTR-8/SVneo cells (**H**–**K**). The red fluorescence is JC1 monomer, and the green signal is JC1 monomer. The morphology of mitochondria in each group was observed using transmission electron microscopy (**L**, **M**). Black arrows represent mitochondrial swelling and disappearance of mitochondrial cristae, and red arrows represent mitochondrial membrane rupture. Flow cytometry was used to detect the degree of cell apoptosis (**N**), and the apoptosis rate of each group was calculated (**O**), where apoptotic cells = early apoptotic cells and mid-stage apoptotic cells. * indicates $p < 0.05$, ** indicates $p < 0.01$, *** indicates $p < 0.001$, and **** indicates $p < 0.0001$.

Having clarified the beneficial effects of melatonin on embryo implantation, we further verified its functional effects on HTR-8/SVneo human trophoblast cells. Similar to the aforementioned findings, melatonin effectively promoted cell proliferation, inhibited apoptosis, enhanced cell migration, and helped to maintain oxidative stress homeostasis. Further analysis of the effects of melatonin on the transcriptome of trophoblast cells showed that DEGs were enriched in terms such as "mitochondrial function", "oxidative phosphorylation", "improved response to hypoxia", and "cell adhesion". This suggests that the ability of melatonin to improve oxidative stress resistance and adhesion functions in trophoblast cells might be the basis for its role in promoting embryo implantation.

After analyzing the transcriptome sequencing results and screening for potential target genes of melatonin, GDF15 became one focus. GDF15 belongs to the transforming growth factor beta superfamily, which regulates gene expression mainly by activating the SMAD family of transcription factors[37]. GDF15 is associated with a variety of pathological and physiological processes, including inflammation, pregnancy, energy metabolism, and tumorigenesis[38–40]. During normal pregnancy, GDF15 is highly expressed in the placenta[41], and its reduced expression is associated with various pregnancy complications, including early miscarriage, preeclampsia, and diabetes[42]. Studies have shown that GDF15 levels in the serum and trophoblast tissues of pregnant women who miscarried are significantly lower than those in women with live birth[20], and the injection of recombinant GDF15 significantly reduced the rate of abortion in mice[43], suggesting that GDF15 is closely related to embryo implantation and early embryonic development.

EMT is a complex, coordinated, and dynamic process characterized by the downregulation of E-CAD and the upregulation of N-CAD[44]. During embryo implantation, the trophectoderm has been shown to exhibit low expression of the tight junction molecule E-CAD and enhanced expression of mesenchymal markers, such as N-CAD and VIMENTIN[45], whereas the abnormal regulation of E-CAD and N-CAD can lead to implantation failure[46,47]. In this study, we demonstrated that melatonin significantly promoted GDF15 expression in human trophoblast cells and further regulated N-CAD and E-CAD expression by activating the SMAD2/3 signaling pathway, which induced cellular EMT, thereby improving migration and promoting embryo implantation.

Studies have demonstrated that when cells are subjected to oxidative stress, inflammation, and ferroptosis, the antioxidant effects of GDF15 can significantly influence the onset and progression of various diseases. For instance, Wang et al. found that overexpression of GDF15 prevents hepatic steatosis by inhibiting the overproduction of ROS[48]; Chen et al. demonstrated

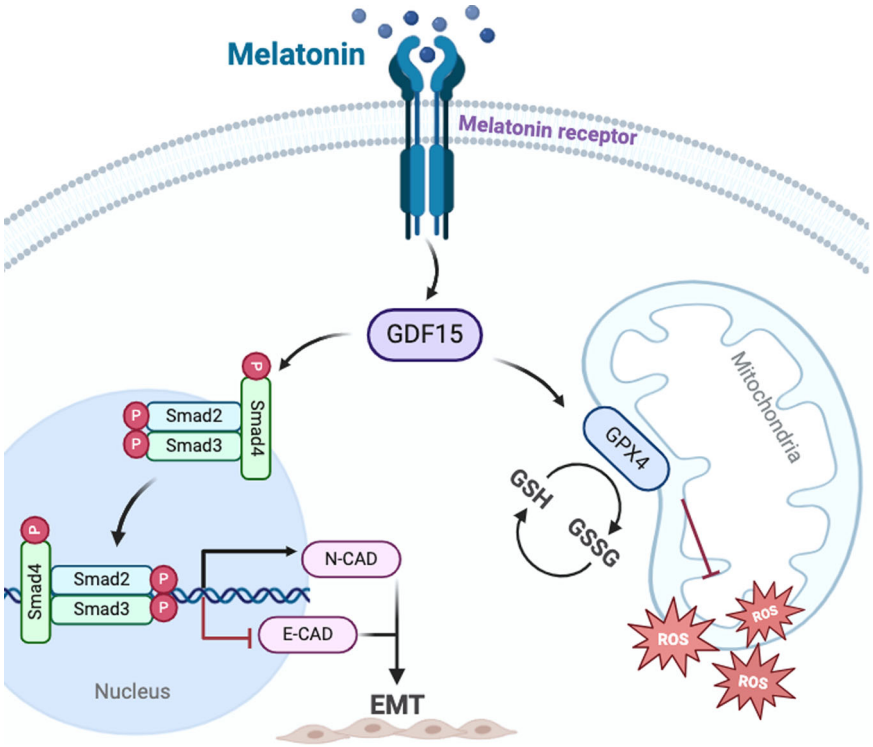

Fig. 10 | Melatonin regulates trophoblast cell function and embryonic implantation by promoting GDF15. This figure is created in BioRender. Guang, Y. (2025) https://BioRender.com/q63k051.

that knocking down GDF15 results in reduced expression of SLC7A11, which subsequently increases cellular peroxide levels and leads to lipid peroxidatio[49]; and Li et al. reported that melatonin alleviates ferroptosis by modulating GDF15, thereby improving hormonal osteonecrosis of the femoral head[50]. During embryonic development, pre-implantation embryos are frequently subjected to the hypoxic conditions of the female reproductive tract[51], which, when combined with specific factors like delayed implantation, can result in excessive ROS and negatively impact subsequent embryonic development. Therefore, a deeper understanding of the regulatory mechanisms of ROS during embryonic development is beneficial for improving conditions such as early miscarriage and delayed implantation. Our findings suggest that melatonin can reduce ROS production and protect mitochondrial functions in trophoblast cells through GDF15-GPX4 pathway.

Our study innovatively revealed that melatonin influences the EMT of trophoblast cells through the GDF15-SMAD2/3 signaling pathway and further elucidated the critical role of the Mel-GDF15-GPX4 axis in combating oxidative stress (Fig. 10), which not only enriches the antioxidant mechanisms of melatonin but also highlights the critical role of GDF15 during embryo implantation.

Materials and methods

Experimental ethics and sample collection

The study was conducted in accordance with the Laboratory animal-Guideline for ethical review of animal welfare and Measures for Ethical Review of Biomedical Research Involving Humans of China. This study has been approved by the Ethics Committee of the First Affiliated Hospital of Zhengzhou University (approval number 2021-KY-0868-002).

The human embryo samples were developed from abnormal fertilized zygotes from patients undergoing in vitro fertilization-embryo transfer treatment in our center. The inclusion criteria included: age≤35, normal chromosomes of both parties; the exclusion criteria included: age>35, ovarian hypofunction, chromosomal abnormalities, combined with hyperprolactinemia, thyroid dysfunction and other endocrine diseases, previous pelvic or ovarian surgery patients with medical history, infectious disease history, family genetic history, and systemic diseases. An informed consent form was signed to agree that the embryos would be discarded for scientific research purposes. All ethical regulations relevant to human research participants were followed.

KM mice (8 weeks) were purchased from Vital Lever (Beijing, China). We have complied with all relevant ethical regulations for animal use.

In vitro embryo culture

Human D5 blastocysts or mouse E3.5 blastocysts were obtained and then randomly assigned to groups. The zona pellucida was removed using Tyrode's solution (Sigma-Aldrich, MO, USA) and then moved into an 8-well plate (Ibidi, WI, USA) cultured in the incubator. Human blastocysts were cultured to D8 using IVC1; mouse E3.5 blastocysts were cultured to E5.5 using IVC1, then the culture medium was replaced with IVC2 and culture to E6.5. The in vitro culture method was as described in previous research[52,53].

The components of the IVC1 culture medium were as follows: Advanced DMEM/F12 (Thermo Fisher Scientific) + 20% (v/v) DFBS (Thermo Fisher Scientific) + 1×ITS-X (Thermo Fisher Scientific) + 200 ng/mL progesterone (Sigma-Aldrich, St. Louis, MO, USA) + 8 nM β-estradiol (Sigma-Aldrich) + 25 μM *N*-acetylcysteine (Sigma-Aldrich) + 0.22% (v/v) sodium lactate (Sigma-Aldrich) + 2 mM L-glutamine (Thermo Fisher Scientific) + 10 μM Y27632 (Selleck, Shanghai, China) + 1 mM sodium pyruvate (Sigma-Aldrich).

The components of the IVC2 culture medium were as follows: Advanced DMEM/F12 + 30% (v/v) KOSR (Thermo Fisher Scientific) + 1× ITS-X + 200 ng/mL progesterone + 8 nM β-estradiol + 25 μM *N*-acetylcysteine + 0.22% (v/v) sodium lactate + 2 mM L-glutamine + 10 μM Y27632 + 1 mM sodium pyruvate + 10% Matrigel (Corning, NY, USA).

Mouse early pregnancy model

Each female mouse was injected intraperitoneally with 10 IU PMSG, and 48 h later with 10 IU hCG. They were caged with male mice at a ratio of 1:3 at 17:00 that night. The next day, the female mice were randomly divided into control group, melatonin group and the luzindole group, the drug was injected continuously for 7 days starting from E0.5. Among them, the injection dose of melatonin (HY-B0075, MCE, Shanghai, China) was 10 mg/kg, the injection dose of melatonin receptor inhibitor luzindole (S3584, Selleck, Shanghai, China) was 1 mg/kg, and the mice in the control

group were injected equal volume of normal saline (with 1/100 DMSO). At E7.5, the mouse uterus was obtained to observe the number of embryo implantation sites, and the decidual tissue or embryonic tissue was peeled off for subsequent detection.

HTR-8/SVneo cell culture and treatment

Cells were cultured in RPMI 1640 (Thermo Fisher Scientific, MA, USA) supplemented with 10% fetal bovine serum (HyClone, UT, USA), 100 U/mL penicillin, and 10 μg/mL streptomycin sulfate (HyClone) in an incubator at 37 °C and 5% CO2. HTR8/Svneo cells were treated with melatonin at concentrations of 0, 10, 50, and 100 μM for 6 h or 24 h, H_2O_2 at 0, 250, 500, 800, 1000 μM for 2 h, and SIS3 (HY13013, MCE) at 5 μM for 6 h.

siRNA transfection

Cells were seeded in 6-well plates. When the cells reached 70% confluence, the culture medium was replaced with RPMI 1640, and the transfection reagent mixture containing Opti-MEM (Thermo Fisher Scientific), Lipofectamine 2000 (Thermo Fisher Scientific), and siRNA (GenePharma, Shanghai, China) was added dropwise into each well. After 6 h, the culture medium was replaced with the normal culture medium. GDF15–1 siRNA, 5′-ACGGUGAAUGGCUCUCAGATT-3′ (sense) and 5′- UCUGAGAGC CAUUCACCGUTT-3′ (antisense) ; GDF15–2 siRNA, 5′- GGAUACUC ACGCCAGAAGUTT-3′ (sense) and 5′-ACUUCUGGCGUGAGUAUCC TT-3′ (antisense); GDF15–3 siRNA, 5′- ACCAACUGCUGGCAGAAUC TT-3′ (sense) and 5′- GAUUCUGCCAGCAGUUGGUTT-3′ (antisense).

Real-Time PCR

Cells were lysed using TRIzol (Invitrogen, CA, USA) and total cellular RNA was extracted. RNA was reverse transcribed to cDNA using RT Kit (Bio-Rad Laboratories, CA, USA). Real-time PCR was performed on a 7500 Real-Time PCR System (Bio-Rad Laboratories) using SYBR Green SuperMix (Bio-Rad Laboratories), and the $2^{-\triangle\triangle Ct}$ method was used to calculate the relative expression level of the target gene. The gene primer sequences involved in this research are in Supplementary Table S1.

Western blot

Cellular proteins were lysed using RIPA (Sangon Biotech, Shanghai, China). Equivalent amounts of protein were separated by SDS-PAGE and transferred to a PVDF membrane. After blocking with 5% milk for 1 h, the primary antibody was incubated overnight in 4°C. GDF15 (27455-1-AP, anti-rabbit, Proteintech, Wuhan, China, 1:1000), E-CAD (20874-1-AP, anti-rabbit, Proteintech, 1:1000), N-CAD (22018-1-AP, anti-rabbit, Proteintech, 1:1000), GPX4 (381958, Zen-bioscience, Chengdu, China 1:1000), SMAD2/3 (8685, anti-rabbit, Cell signaling technology, MA, USA, 1:1000), SMAD1 (6944, anti-rabbit, Cell signaling technology, 1:1000), SMAD5 (12534, anti-rabbit, Cell signaling technology, 1:1000), p-SMAD3 (9520, anti-rabbit, Cell signaling technology, 1:1000), p-SMAD1/5 (13820, anti-rabbit, Cell signaling technology, 1:1000), B-ACTIN (AP0060, anti-rabbit, Bioworld, Nanjing, China, 1:8000), GAPDH (AP0063, anti-rabbit, Bioworld, 1:8000). On the following day, the membranes were incubated with the secondary antibody. The immunoreactive bands were detected using an enhanced chemiluminescent substrate (Bio-Rad Laboratories). Original gel and blot images are shown in Supplementary Figs. 8, 9.

Cell viability detection

The HTR-8/SVneo cell line was counted in advance and evenly seeded in a 96-well plate at a density of 5×10^4/well. After 96 h of drug treatment, the culture medium was discarded, RPMI 1640 and CCK-8 solution (AR1160, Boster Biological Technology, Wuhan, China) were mixed at a ratio of 10:1 and added to a 96-well plate, and incubated in a 37 °C incubator for 120 min, and detect the absorbance at 450 nm on a microplate reader.

Mitochondrial membrane potential detection

To detect mitochondrial membrane potential (MMP), cells were cultured at 37 °C for 30 min in the medium containing 2 μM JC-1 (C2006, Beyotime, Shanghai, China). Photos were taken using a Zeiss confocal microscope (Carl Zeiss, Oberkochen, Germany).

ROS detection

To measure the level of ROS, cells were incubated at 37 °C for 30 min in the culture medium containing 10 mM carboxy-H2DCF diacetate (S0033S, Beyotime). After washed with PBS for 3 times, the cells were imaged with a confocal microscope (Carl Zeiss) or measured the fluorescence intensity at 488 nm with a fluorescent microplate reader.

Cell immunofluorescence

Cells were fixed with 4% PFA and then permeabilized by 0.5% Triton X-100. 5% BSA was added to block cells and then incubate the cells in primary antibody at 4 °C overnight. MT1 (bs0027r, anti-rabbit, Bioss Antibodies, Beijing, China, 1:1000), MT2 (bs0027r, anti-rabbit, Bioss Antibodies, 1:1000). Remove the primary antibodies the next day and incubate the secondary antibody at room temperature for 30 min, the cells were placed in DAPI solution and photographed under the confocal microscope (Carl Zeiss, Oberkochen, Germany).

Flow cytometry

The cells were seeded in advance in a 6-well plate, and the drug was added when the cell density reaches 60%-70%. After the treatment, EDTA-free trypsin was used to digest and collect the cells.

When cell apoptosis was measured, Binding Buffer (KeyGen Biotech, Nanjing, China) was used to suspend the cells, Annexin V-FITC (KeyGen Biotech) and Propidium Iodide (KeyGen Biotech) were added in sequence. After reacting for 5–15 min at room temperature, the BD Accuri C6 Plus flow cytometer (BD Biosciences, CA, USA) was used for flow cytometry analysis, and FlowJo 10.4 (BD Biosciences) was used to analyze the different stages of apoptosis percentage of cells.

When cell cycle was measured, pre-cooled 70% ethanol was added and fix the cell overnight at 4 °C. The next day, PI/RNase (KeyGen Biotech) solution was added for 30 min. Cell cycle determination was performed using a BD Accuri C6 Plus flow cytometer (BD Biosciences), and the percentage of cells in different cell cycles was analyzed using FlowJo 10.4 (BD Biosciences). The gating strategy is shown in Supplementary Figs. 4-7.

Transcriptome sequencing

Total RNA from the samples was extracted using TRIzol, and genomic DNA was removed by DNaseI (TaKara, Beijing, China). 2100 Bioanalyser (Agilent Technologies, CA, USA) and ND-2000 (NanoDrop Technologies, DE, USA) were used to detect the quality of RNA samples. Samples with qualified quality (OD260/280 = 1.8–2.2, OD260/230 ≥ 2.0, RIN ≥ 6.5, 28S:18S ≥ 1.0, >1 μg) will be subjected to transcriptome sequencing. The library was established using TruSepTM RNA sample preparation Kit (Illumina, CA, USA). High-throughput sequencing was performed using the Illumina HiSeq xten/NovaSeq 6000 sequencing platform, with a sequencing read length of PE150.

Scratch assay

Use a marker pen to draw horizontal lines evenly on the back of the 6-well plate, with at least 5 horizontal lines crossing each hole. Add approximately 5×10^5 cells to the well, and use the pipette tip to scratch the well vertically the next day. Wash three times with PBS, add serum-free medium and place in an incubator to continue culturing. Samples will be taken and photographed at 0, 6, 12 and 24 h.

Transwell migration assay

Drug-treated cells were collect the resuspend in serum-free medium. 600 μL of serum-containing culture medium was added to the lower chamber of the 24-well plate, and 200 μL of cell suspension was added to the upper chamber of the 24-well plate. After culturing for 6–12 h, remove the Transwell chamber, wash twice with PBS, fix with 4% PFA for 30 min, and stain with 0.1% crystal violet for 20 min. Use a cotton swab to gently wipe off the non-

migrated cells in the upper layer and wash it 3 times with PBS, then randomly select five fields of view to observe the cells under a microscope and count them.

Immunohistochemistry

The mouse tissue was fixed with 4% PFA, embedded in paraffin, and sectioned at every 5 μm thickness. The embryonic interface was selected for staining: the sections were baked in a 65 °C incubator for 1 h and then placed in xylene. Antigen retrieval was performed after sections were treated with graded alcohol. Add an appropriate amount of 3% hydrogen peroxide solution, incubate at room temperature for 10 min, then wash with PBS and incubate with 5% BSA for 110 min. After pouring off the liquid, add the primary antibody and incubate at 4 °C overnight. The next day, the primary antibody was washed three times with PBS, then the corresponding secondary antibody was added, and incubated at 37 °C. After incubation for 1 h, the sections were stained with DAB, counterstained with hematoxylin for 20 s, and sealed with neutral gum. The photos were taken for observation.

Statistics and reproducibility

Statistical analysis of data was performed using SPSS 22.0. Normally distributed continuous variables are expressed as "mean ± standard deviation". Comparisons between the two groups were performed using the parametric Student's *t* test or the nonparametric Mann–Whitney *U* test, and the chi-square test was used for comparisons between categorical variables. The difference was considered statistically significant when $p < 0.05$, and each experiment was independently repeated three or more times.

Reporting summary

Further information on research design is available in the Nature Portfolio Reporting Summary linked to this article.

Data availability

Numerical source data for all graphs in the manuscript can be found in Supplementary Data 1 file. Gating strategy (Supplementary Figs. 4–7) for flow cytometry and uncropped and unedited blot/gel images (Supplementary Figs. 8, 9) can be found in the Supplementary Information pdf. The accession code for the RNA-seq data is PRJNA1219531. All other data are available from the corresponding author on reasonable request.

Received: 22 July 2024; Accepted: 26 February 2025;
Published online: 08 March 2025

References

1. Kim, S. M. & Kim, J. S. A review of mechanisms of implantation. *Dev. Reprod.* **21**, 351–359 (2017).
2. Zhang, S. et al. Physiological and molecular determinants of embryo implantation. *Mol. Asp. Med.* **34**, 939–980 (2013).
3. Oghbaei, F. et al. Epithelial-mesenchymal transition process during embryo implantation. *Cell Tissue Res.* **388**, 1–17 (2022).
4. Hannon, T., Innes, B. A., Lash, G. E., Bulmer, J. N. & Robson, S. C. Effects of local decidua on trophoblast invasion and spiral artery remodeling in focal placenta creta - an immunohistochemical study. *Placenta* **33**, 998–1004 (2012).
5. Khokhlova, E. V., Fesenko, Z. S., Sopova, J. V. & Leonova, E. I. Features of DNA repair in the early stages of mammalian embryonic development. *Genes (Basel)* **11**, 1138 (2020).
6. Musson, R., Gąsior, Ł., Bisogno, S. & Ptak, G. E. DNA damage in preimplantation embryos and gametes: specification, clinical relevance and repair strategies. *Hum. Reprod. Update* **28**, 376–399 (2022).
7. Ornoy, A. Embryonic oxidative stress as a mechanism of teratogenesis with special emphasis on diabetic embryopathy. *Reprod. Toxicol.* **24**, 31–41 (2007).
8. Nowaczyk, J., Poniedziałek, B., Rzymski, P., Sikora, D. & Ropacka-Lesiak, M. Platelets in fetal growth restriction: role of reactive oxygen species, oxygen metabolism, and aggregation. *Cells* **11**, 724 (2022).
9. Liang, Y. et al. 1-Nitropyrene exposure impairs embryo implantation through disrupting endometrial receptivity genes expression and producing excessive ROS. *Ecotoxicol. Environ. Saf.* **227**, 112939 (2021).
10. Eker, C., Basdas, R., Balci, B. K., Bastu, E. & Gunel, T. The genomic analysis of endometrial mitochondrial DNA copy number variation on recurrent implantation failure. *J. Gynecol. Obstet. Hum. Reprod.* **50**, 101945 (2021).
11. Sheikhansari, G. et al. Oxidative stress, inflammatory settings, and microRNA regulation in the recurrent implantation failure patients with metabolic syndrome. *Am. J. Reprod. Immunol.* **82**, e13170 (2019).
12. Reiter, R. J. The melatonin rhythm: both a clock and a calendar. *Experientia* **49**, 654–664 (1993).
13. Carlomagno, G., Minini, M., Tilotta, M. & Unfer, V. From Implantation to Birth: Insight into Molecular Melatonin Functions. *Int J. Mol. Sci.* **19**, 2802 (2018).
14. Zhang, L. et al. Effects of melatonin administration on embryo implantation and offspring growth in mice under different schedules of photoperiodic exposure. *Reprod. Biol. Endocrinol.* **15**, 78 (2017).
15. He, C. et al. Melatonin-related genes expressed in the mouse uterus during early gestation promote embryo implantation. *J. Pineal Res.* **58**, 300–309 (2015).
16. Lanoix, D., Lacasse, A. A., Reiter, R. J. & Vaillancourt, C. Melatonin: the smart killer: the human trophoblast as a model. *Mol. Cell Endocrinol.* **348**, 1–11 (2012).
17. Ma, X. et al. The uterine melatonergic systems of AANAT and melatonin membrane receptor 2 (MT2) are essential for endometrial receptivity and early implantation in mice. *Int. J. Mol. Sci.* **24**, 7127 (2023).
18. Liu, Z., Chen, B., Chang, J., Feng, L. & Zhao, X. Melatonin regulates trophoblast pyroptosis, invasion and migration in preeclampsia by inhibiting HtrA1 transcription through the microRNA-520c-3p/SETD7 axis. *Am. J. Reprod. Immunol.* **87**, e13523 (2022).
19. Bae, H. et al. Melatonin improves uterine-conceptus interaction via regulation of SIRT1 during early pregnancy. *J. Pineal Res.* **69**, e12670 (2020).
20. Zeng, Y. T., Liu, W. F., Zheng, P. S. & Li, S. GDF15 deficiency hinders human trophoblast invasion to mediate pregnancy loss through downregulating Smad1/5 phosphorylation. *iScience* **26**, 107902 (2023).
21. Carrillo-Vico, A., Guerrero, J. M., Lardone, P. J. & Reiter, R. J. A review of the multiple actions of melatonin on the immune system. *Endocrine* **27**, 189–200 (2005).
22. Ekmekcioglu, C. Melatonin receptors in humans: biological role and clinical relevance. *Biomed. Pharmacother.* **60**, 97–108 (2006).
23. Claustrat, B., Brun, J. & Chazot, G. The basic physiology and pathophysiology of melatonin. *Sleep. Med. Rev.* **9**, 11–24 (2005).
24. Reiter, R. J. et al. Melatonin and reproduction revisited. *Biol. Reprod.* **81**, 445–456 (2009).
25. Wang, Y. et al. Melatonin levels and embryo quality in IVF patients with diminished ovarian reserve: a comparative study. *Reprod. Biol. Endocrinol.* **22**, 127 (2024).
26. Qu, P. et al. Extracellular vesicles and melatonin benefit embryonic develop by regulating reactive oxygen species and 5-methylcytosine. *J. Pineal Res.* **68**, e12635 (2020).
27. Lanoix, D., Beghdadi, H., Lafond, J. & Vaillancourt, C. Human placental trophoblasts synthesize melatonin and express its receptors. *J. Pineal Res.* **45**, 50–60 (2008).
28. Iwasaki, S. et al. Melatonin as a local regulator of human placental function. *J. Pineal Res.* **39**, 261–265 (2005).
29. García, J. J. et al. Protective effects of melatonin in reducing oxidative stress and in preserving the fluidity of biological membranes: a review. *J. Pineal Res.* **56**, 225–237 (2014).
30. Sharma, A. & Zheng, B. Melatonin mediated regulation of drought stress: physiological and molecular aspects. *Plants (Basel)* **8**, 190 (2019).

31. Ma, C. et al. Melatonin mitigates PNMC-induced disruption of spindle assembly and mitochondrial function in mouse Oocytes. *Ecotoxicol. Environ. Saf.* **282**, 116703 (2024).
32. Shi, X. Y. et al. Melatonin ameliorates the toxic effects of 2,6-dichloro-1,4-benzoquinone on mouse oocytes by restoring subcellular structures. *Ecotoxicol. Environ. Saf.* **288**, 117421 (2024).
33. Su, X. et al. Melatonin protects porcine oocytes from gossypol-induced meiosis defects via regulation of SIRT1-mediated mitophagy. *Food Chem. Toxicol.* **195**, 115122 (2025).
34. Nadri, P., Zahmatkesh, A. & Bakhtari, A. The potential effect of melatonin on in vitro oocyte maturation and embryo development in animals. *Biol. Reprod.* **111**, 529–542 (2024).
35. Soliman, A. et al. Placental melatonin system is present throughout pregnancy and regulates villous trophoblast differentiation. *J. Pineal Res.* **59**, 38–46 (2015).
36. Sagrillo-Fagundes, L., Assunção Salustiano, E. M., Ruano, R., Markus, R. P. & Vaillancourt, C. Melatonin modulates autophagy and inflammation protecting human placental trophoblast from hypoxia/reoxygenation. *J. Pineal Res.* **65**, e12520 (2018).
37. Gough, N. R., Xiang, X. & Mishra, L. TGF-β signaling in liver, pancreas, and gastrointestinal diseases and cancer. *Gastroenterology* **161**, 434–452.e415 (2021).
38. Luan, H. H. et al. GDF15 is an inflammation-induced central mediator of tissue tolerance. *Cell* **178**, 1231–1244.e1211 (2019).
39. Fejzo, M. S. et al. Nausea and vomiting of pregnancy and hyperemesis gravidarum. *Nat. Rev. Dis. Prim.* **5**, 62 (2019).
40. Lockhart, S. M., Saudek, V. & O'Rahilly, S. GDF15: a hormone conveying somatic distress to the brain. *Endocr. Rev.* **41**, bnaa007 (2020).
41. Yokoyama-Kobayashi, M., Saeki, M., Sekine, S. & Kato, S. Human cDNA encoding a novel TGF-beta superfamily protein highly expressed in placenta. *J. Biochem.* **122**, 622–626 (1997).
42. Chen, Q. et al. Serum levels of GDF15 are reduced in preeclampsia and the reduction is more profound in late-onset than early-onset cases. *Cytokine* **83**, 226–230 (2016).
43. Lyu, C. et al. Insufficient GDF15 expression predisposes women to unexplained recurrent pregnancy loss by impairing extravillous trophoblast invasion. *Cell Prolif.* **56**, e13514 (2023).
44. Cavallaro, U., Schaffhauser, B. & Christofori, G. Cadherins and the tumour progression: is it all in a switch? *Cancer Lett.* **176**, 123–128 (2002).
45. Yamakoshi, S. et al. Expression of mesenchymal-related genes by the bovine trophectoderm following conceptus attachment to the endometrial epithelium. *Reproduction* **143**, 377–387 (2012).
46. Gilbert, J. S., Bauer, A. J., Gingery, A., Banek, C. T. & Chasson, S. Circulating and utero-placental adaptations to chronic placental ischemia in the rat. *Placenta* **33**, 100–105 (2012).
47. Reardon, S. N. et al. CDH1 is essential for endometrial differentiation, gland development, and adult function in the mouse uterus. *Biol. Reprod.* **86**, 141–110 (2012). 141.
48. Wang, Y. et al. Overexpression of NAG-1/GDF15 prevents hepatic steatosis through inhibiting oxidative stress-mediated dsDNA release and AIM2 inflammasome activation. *Redox Biol.* **52**, 102322 (2022).
49. Chen, L., Qiao, L., Bian, Y. & Sun, X. GDF15 knockdown promotes erastin-induced ferroptosis by decreasing SLC7A11 expression. *Biochem. Biophys. Res. Commun.* **526**, 293–299 (2020).
50. Li, W. et al. Exogenous melatonin ameliorates steroid-induced osteonecrosis of the femoral head by modulating ferroptosis through GDF15-mediated signaling. *Stem Cell Res Ther.* **14**, 171 (2023).
51. Daikoku, T. et al. Expression of hypoxia-inducible factors in the peri-implantation mouse uterus is regulated in a cell-specific and ovarian steroid hormone-dependent manner. Evidence for differential function of HIFs during early pregnancy. *J. Biol. Chem.* **278**, 7683–7691 (2003).
52. Bedzhov, I., Leung, C. Y., Bialecka, M. & Zernicka-Goetz, M. In vitro culture of mouse blastocysts beyond the implantation stages. *Nat. Protoc.* **9**, 2732–2739 (2014).
53. Shahbazi, M. N. et al. Self-organization of the human embryo in the absence of maternal tissues. *Nat. Cell Biol.* **18**, 700–708 (2016).

Acknowledgements

The authors thank all the patients involved in this study, and the staff in our center. This study was supported by National Natural Science Foundation of China (32370917 to Yingpu Sun; U1904138 to Guidong Yao), Open Research Fund of National Health Commission Key Laboratory of Birth Defects Prevention (NHCKLBDP202407 to Guidong Yao), and Zhengzhou University School of Medical Sciences Clinical First-class Subject Talent Cultivation Project (to Guidong Yao).

Author contributions

Guang Yang: Investigation, Data Curation, Writing—Original Draft; Guidong Yao: Methodology,Writing—Review & Editing, Supervision, Funding acquisition; Huihui Wang, Ran Jiang: Investigation, Data Curation; Junnan Fang, Jingyi Hu, Yue Kong: Investigation, Data Curation; Haixia Jin, Wenyan Song, Zhaoting Wu, Xianju Huang: Resources, Data Curation; Yingpu Sun: Writing - Review & Editing, Supervision, Funding acquisition.

Competing interests

The authors declare no competing interests.

Additional information

Supplementary information The online version contains supplementary material available at https://doi.org/10.1038/s42003-025-07834-1.

Correspondence and requests for materials should be addressed to Guidong Yao or Yingpu Sun.

Peer review information *Communications Biology* thanks Erica L. Johnson and the other, anonymous, reviewer(s) for their contribution to the peer review of this work. Primary Handling Editor: Christina Karlsson Rosenthal.